ELSEVIER

Journal of Nuclear Materials 246 (1997) 189–195

journal of nuclear materials

# Hot hardness and indentation creep studies on Zr–1Nb–1Sn–0.1Fe alloy

T.R.G. Kutty [a,*], T. Jarvis [a], C. Ganguly [b]

[a] *Radiometallurgy Division, Bhabha Atomic Research Centre, Trombay, Bombay 400 085, India*
[b] *Central Glass and Ceramic Research Institute, Jadavpur, Calcutta 700 032, India*

Received 16 December 1996; accepted 24 April 1997

**Abstract**

The hot hardness behaviour of the Zr–1Nb–1Sn–0.1Fe alloy was evaluated from room temperature to 1173 K at 100 K intervals. The hardness versus temperature data for this alloy can be represented by the relationship $H = \kappa \exp(-BT)$. The indentation creep measurements of the above mentioned alloy were carried out using a load of 300 g at 573, 673, 773, 873 and 973 K. The stress exponent obtained from hardness–time plots was found to be temperature dependant and decreases from a value of nearly 42 at 573 K to ~5 at 973 K. The activation energy for creep was also found to be temperature dependant for this alloy. At least four different domains of creep were observed in the temperature range of 573–973 K. The mechanism in the temperature regime of 573–673 K was found to be athermal. © 1997 Elsevier Science B.V.

## 1. Introduction

The Zr–1Nb–1Sn–0.1Fe alloy is an advanced cladding material for nuclear fuel elements in water cooled reactors. In a typical pressurized heavy water reactor (PHWR) of 220 MW capacity, there are more than 100,000 fuel elements undergoing irradiation at a time. A primary life limiting factor for the conventional zirconium alloys (Zircaloy-2 and Zircaloy-4) in a nuclear reactor is postulated to be corrosion in hot natural or heavy water. With a view to improving the performance of Zr alloys for cladding, which can withstand a higher burn up, several alloys have been developed. The alloy of Zr–1Nb–1Sn–0.1Fe (composition in wt%) has shown excellent corrosion resistance and superior irradiation performance [1,2]. It has been reported that the corrosion rate of the above mentioned alloy is only 60% of that of Zircaloy-4 and the irradiation creep and irradiation growth of the above is only 80 and 60%, respectively, of that of Zircaloy-4 [3]. Although the Zr–1Nb–1Sn–0.1Fe alloy has a good potential for use as nuclear fuel cladding, many of its properties are not fully investigated.

One of the major reasons for utilizing Zr base alloys in nuclear reactors is its resistance to creep. Although, the major source of deformation in Zr components in water cooled reactors is irradiation creep, the thermal creep is also expected to give rise to significant deformation in these components [4]. Moreover, the thermal creep behaviour is intimately related to the irradiation creep and therefore, an understanding of irradiation creep in Zr alloys necessitates a thorough knowledge of its thermal creep behaviour as well. Finally, an understanding of thermal creep provides some incentives in quality control and quality assurance of reactor core components [4,5].

The variation of hardness with temperature is similar to the variation of yield stress with temperature since hardness is intimately related to the yield stress [6–8]. Therefore, the determination of hardness at high temperature has been often resorted to as a tool to collect information on high temperature strength properties and also to understand the softening behaviour of materials. In this paper, the hot hardness of Zr–1Nb–1Sn–0.1Fe alloy has been presented from room temperature to 1173 K and the indentation creep behaviour of this alloy has been evaluated over a temperature range of 573–973 K. The hardness creep test

* Corresponding author.


*PII* S0022-3115(97)00108-6

provides a simple and non-destructive method of investigating the mechanical properties of a solid. In this test, the indenter is maintained at a constant load over a period of time under well controlled conditions. As the stresses cause the material beneath the indenter to creep, the indenter penetrates the material and the changes in the indentation size are measured.

## 2. Experimental

The alloy was obtained from Nuclear Fuel Complex, Hyderabad, in the form of a sheet of about 1 mm in thickness. The sheet had been made by the hot extrusion of the arc melted alloy followed by a series of hot and cold rolling steps with intermediate vacuum annealing processes. The sheet was finally annealed at 973 K for 1 h. The chemical composition of the alloy is presented in Table 1.

The hot hardness measurements were carried out using a Nikon hot hardness tester with the help of a diamond Vickers microhardness indenter. For this, samples of 5 × 5 mm were cut from the sheets and were metallographically prepared. The sample was loaded into the furnace of the hot hardness tester and evacuated to 0.1 Pa. Fig. 1 schematically illustrates the plane and the location on which hardness measurements were carried out. All the indentations were located near the centre of the surface as shown in the figure. The hardness was measured from room temperature to 1173 K at 100 K intervals using 300 g load and a dwell time of 5 s. At each temperature, at least 5 indentations were taken and the hardness was calculated using the relation

$$H = 1854.4 \times P/d^2, \quad (1)$$

where $P$ is the load (g) and $d$ is the average diagonal ($\mu$m).

The indentation creep measurements were carried out using a load of 300 g at 573, 673, 773, 873 and 973 K. The load was applied at a rate of 0.3 mm/min. At each temperature, the hardness was measured as a function of dwell time. The dwell times used in this study were 1, 5, 10, 30, 100, 300 and 1000 s and were measured within ±0.1 s. For each dwell time, at least 3 indentations were taken. The indentation creep was also measured in the central region of the sample. All the indentations were at least 0.2 mm away from the edges.

The hardness and creep of Zr and its alloys is dependant on texture. The texture produced during fabrication introduces anisotropy in mechanical properties. To reduce the effect of texture, indentations were positioned in such a way that all of them had one of the diagonals parallel to a selected edge of the sample.

Table 1
Chemical analysis of the Zr–1Nb–1Sn–0.1Fe alloy

| Sn (wt%) | Nb (wt%) | Cr (wt%) | Fe (wt%) | O (ppm) | H (ppm) | N (ppm) |
|---|---|---|---|---|---|---|
| 1.08 | 1.10 | 0.018 | 0.098 | 1197 | 9 | 40 |

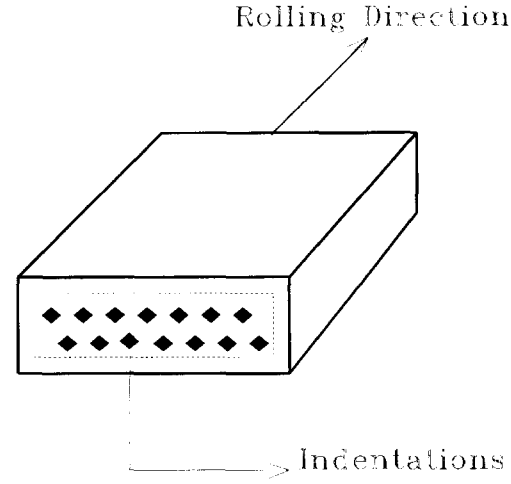


Fig. 1. A schematic of the Zr–1Nb–1Sn–0.1Fe sample showing the plane and locations on which the hot hardness and indentation creep measurements were made.

## 3. Results

The temperature dependence of the hardness of the Zr–1Nb–1Sn–0.1 Fe alloy is shown in Fig. 2. The plot in Fig. 2 shows a gradual decrease in hardness up to ~ 700 K followed by a rapid drop in hardness above that temper-

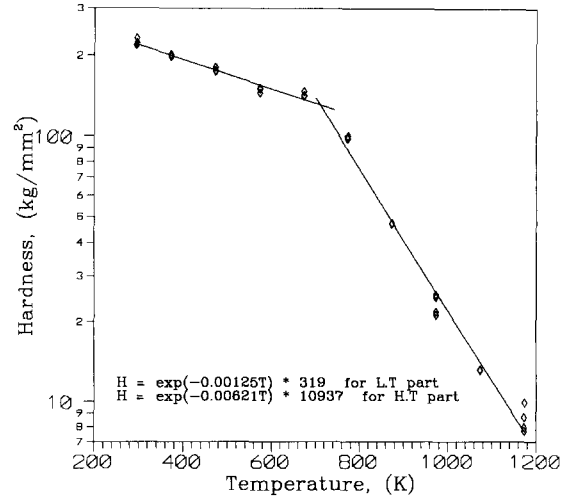


Fig. 2. ln($H$)–temperature plot for the Zr–1Nb–1Sn–0.1Fe alloy showing a transition at 713 K.

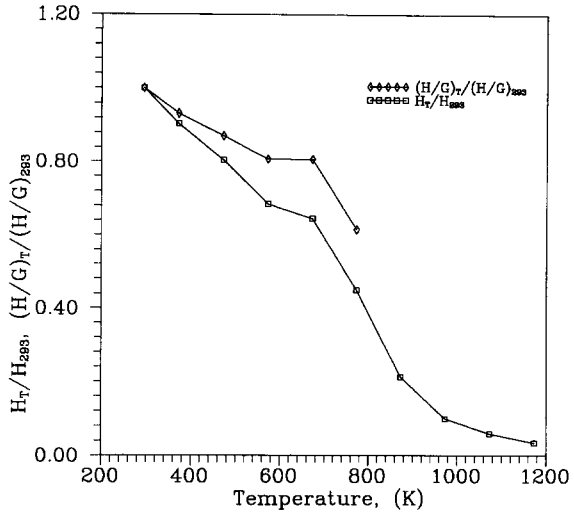


Fig. 3. $H_T/H_{293}$ (where $H_T$ is the hardness at temperature $T$ and $H_{293}$ is the room temperature hardness), against temperature plot for the Zr–1Nb–1Sn–0.1Fe alloy. The $(H/G)_T/(H/G)_{293}$ versus temperature plot is also shown. $G$ is the shear modulus of the alloy.

ature. The graph in Fig. 2 is replotted using $H_T/H_{293}$ (where $H_T$ is the hardness at temperature $T$ and $H_{293}$ is the room temperature hardness) against temperature and is shown in Fig. 3. The hardness falls to ~ 70% of its value at room temperature on attaining 573 K and falls to as low as 3% at 1173 K. The hardness versus time plots at 573, 673, 773, 873 and 973 K are shown in Fig. 4. There is a clear time dependence of hardness in this alloy. This is due to the indentation creep. The interpretation of temperature and time dependence of hardness is discussed in Section 4.

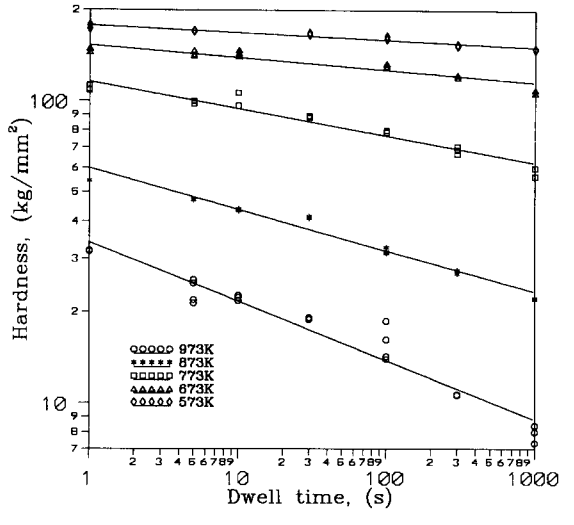


Fig. 4. Hardness–dwell time plots for the Zr–1Nb–1Sn–0.1Fe alloy at 573, 673, 773, 873 and 973 K. The slope of these lines will be $(-1/n)$ from which the stress exponent, $n$, is determined.

## 4. Discussion

### 4.1. Hardness–temperature relationship

The hardness–temperature relationship for metals and alloys was first suggested by Ito [9] and Shishokin [10] and has been explored by a number of investigators [6–8,11,12]. The relation is as given below:

$$H = \kappa \exp(-BT), \tag{2}$$

where $H$ is the hardness, $T$ is the temperature (K), $\kappa$ is called the intrinsic hardness or the value of the hardness at 0 K and $B$ is called the softening coefficient. The constants $\kappa$ and $B$ have one set of values at low temperature and another at high temperature, suggesting a change in the deformation mechanism. The transition between low and high temperature behaviour may occur at one temperature or over a range of temperatures. In most metals and alloys, the transition temperature is known to occur at about $0.5T_m$, where $T_m$ is the melting point.

From the data plotted in Fig. 2, the $H$–$T$ relationship for the Zr–1Nb–1Sn–0.1Fe alloy below and above the transition temperature could be represented by the following relations, respectively:

$$H = 319 \times \exp(-0.00125T), \tag{3}$$

$$H = 10937 \times \exp(-0.00621T), \tag{4}$$

where $H$ is the hardness (kg/mm$^2$) and $T$ is the temperature (K). The transition temperature for the above mentioned alloy was found to be 713 K.

The mechanism controlling the softening at temperatures below the transition temperature for metals and alloys is reported to be slip and deformation twinning [6]. The rate controlling deformation mechanism for pure Zr and its alloys has been studied in detail by compression tests [13]. At low temperature twinning dictates the entire course of plastic deformation whereas above 448 K, slip dominates. In the temperature range 448 to 773 K, α-Zr deforms primarily by slip on $(10\bar{1}0)$ first order prism planes along $\langle 11\bar{2}0\rangle$ direction. The incidence of basal slip has been found to increase with increasing temperature on a basal plane (0001) along $\langle 11\bar{2}0\rangle$ direction [14]. The mechanism of deformation above the transition temperature is diffusional assisted phenomena such as dislocation glide and dislocation climb [6]. A similar mechanism is expected to occur in the case of the Zr–1Nb–1Sn–0.1Fe alloy during deformation.

### 4.2. Indentation creep

Indentation creep is defined as the time dependant motion of a hard indenter into a solid under constant load at a constant temperature [15]. The issues concerning the analysis of indentation creep data has been discussed in the literature [16–20]. The earlier work on indentation creep

was purely empirical or based on various theoretical and numerical approaches. All these different approaches essentially give similar results. In this study, we have adopted the dimensional analysis approach of Sargent and Ashby [21] to analyze the results obtained in this work.

#### 4.2.1. Sargent and Ashby's model of indentation creep [21]

In this model, Sargent and Ashby [21] have suggested that the stress and strain fields in a material below the pyramidal indenter are self similar in time and creep deformation is found to follow the power law of the type

$$\dot{\epsilon} = A'\sigma^n \exp(-Q/RT), \tag{5}$$

where $\dot{\epsilon}$ is the steady state strain rate, $A'$ is a constant, $\sigma$ is the applied stress, $n$ is the stress exponent, $Q$ is the activation energy and $R$ is the universal gas constant.

The displacement rate of an indenter has been derived as

$$du/dt = \left[\dot{\epsilon}_0(\sqrt{A})/C_2\right]\left[(C_1/\sigma_0)(P/A)\right]^n, \tag{6}$$

where $A$ is the projected area of indentation, $C_2$ is a constant and $\dot{\epsilon}_0$ is the strain rate at a reference stress $\sigma_0$.

For a pyramidal indenter the penetration is proportional to $\sqrt{A}$, i.e.,

$$u = C_3\sqrt{A}. \tag{7}$$

Differentiating Eq. (7) with respect to time and substituting into Eq. (6),

$$dA/dt = C_4\dot{\epsilon}_0 A(P/A\sigma_0)^n, \tag{8}$$

where $C_3$ and $C_4$ are constants.

Sargent and Ashby [21] have derived the following relationship between indentation hardness and dwell time:

$$H(t) = (\sigma_0)/(nC_4\dot{\epsilon}_0 t)^{1/n}, \tag{9}$$

where $H(t)$ is the time dependant hardness.

From Eq. (8), when $P$ is held constant, we get

$$(1/H)(dH/dt) = -C_4\dot{\epsilon}_0(H/\sigma_0)^n. \tag{10}$$

Hence, from Eq. (9) the gradient of a plot of $\ln(H)$ against $\ln(t)$ at a constant temperature is $-1/n$. Also a plot of $\ln(H)$ versus $\ln[(-1/H)(dH/dt)]$ at constant temperature has a slope $n$ (from Eq. (10)). The activation energy is calculated from the plot of $\ln(t)$ against $1/T$ at constant hardness, the slope of which provides $Q/R$.

### 4.3. Discussion on indentation creep results

The hardness–time data at various temperatures are analyzed in terms of the dimensional analysis model described above. The hardness versus time data (see Fig. 4) were fitted and slopes were obtained using linear regression analysis. Fig. 5 shows the hardness drop rate $(-1/H)(dH/dt)$ versus hardness plots on a log–log scale.

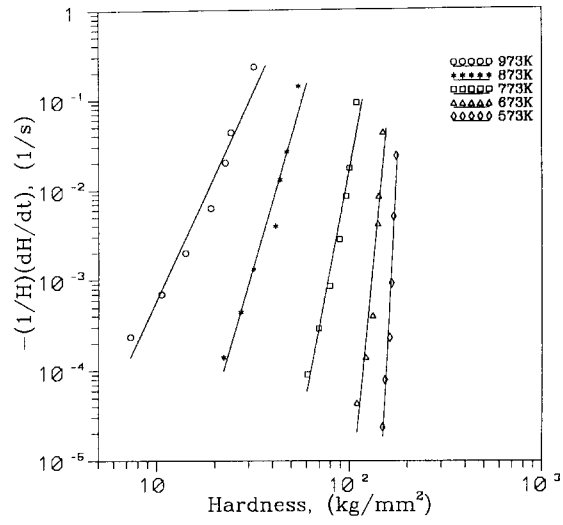


Fig. 5. A plot between $\ln(H)$ and $\ln[(-1/H)(dH/dt)]$ at different temperatures for the Zr–1Nb–1Sn–0.1Fe alloy to determine the stress exponent from the indentation creep data.

The value of stress exponents obtained by both methods are similar and are given in Table 2. It was seen that the stress exponent decreased with temperature from a value of ~42 at 573 K to ~5 at 973 K.

The activation energies calculated from the slope of $\ln(t)$ versus $1/RT$ plots (Fig. 6) are given in Table 3. The data points for this plot are obtained from Fig. 4 by finding the time required to attain a constant hardness at two different temperatures. It can be seen from Table 3 that the activation energy of the Zr–1Nb–1Sn–0.1Fe alloy is temperature dependant.

No data is available in the literature on the creep parameters of the Zr–1Nb–1Sn–0.1Fe alloy whereas exhaustive literature is available on the creep behaviour of Zr and Zircaloy. Gilbert et al. [22] have studied the creep behaviour of pure Zirconium in the temperature range 323 to 1223 K. Five domains of creep behaviour were observed in this temperature regime. The activation energy, stress exponents and the probable mechanism for each domain is given in Table 4 [22]. Shober et al. [23] reported that the

Table 2
The value of stress exponents at different temperatures

| Temperature (K) | Stress exponent, $n$ | |
|---|---|---|
| | using Eq. (9) | using Eq. (10) |
| 573 | 42.5 | 41.8 |
| 673 | 24.6 | 23.9 |
| 773 | 11.2 | 11.2 |
| 873 | 7.8 | 7.4 |
| 973 | 5.3 | 4.7 |

Table 3
Activation energy for creep at different temperatures

| Temperature (K) | Activation energy (kJ/mol) |
|---|---|
| 573–673 | 205 ± 4 |
| 673–773 | 297 ± 3 |
| 773–873 | 418 ± 6 |
| 873–973 | 303 ± 9 |

value of $n$ varied continuously with stress from 1 to a value greater than 100 in Zircaloy-2 for the temperature range 723–773 K. A similar dependence of creep rate on stress has been reported by Bernstein [24] who measured $n$ as a function of stress in Zr and Zircaloy-2. Ardell and Sherby [25], who conducted stress change tests on annealed Zr in the temperature range 923–1123 K, suggested that at high stresses, the stress dependence is better described by an equation of the form

$$\dot{\epsilon} = B' \exp(C\sigma), \tag{11}$$

where $\sigma$ is the applied stress and $B'$ and $C$ are constants.

Holmes [27] reported a temperature dependence of activation energy for Zircaloy-2 in the temperature range 323 to 773 K. He reported that the behaviour of Zircaloy is almost identical to that of pure zirconium. The activation energy was found to increase from about 84 to 243 kJ/mol at a temperature between 323 K and some transition temperature depending on the stress level. A peak in the activation energy was observed around a temperature which was shifted to lower temperatures between 523 and 623 K with increasing stress [28]. A similar peak in the activation energy in the temperature regime 723 to 823 K has been reported by Fidleris [29], Warda et al. [30] and Ramaswami et al. [31] for Zr and Zircaloy. This behaviour was attributed to strain aging of Zr alloys at these temperatures. The activation energy of Zircaloy-2 in the region 773–973 K has been found to be 272 kJ/mol. This value seems to be consistent with the value of 276 kJ/mol obtained for pure Zr in the above mentioned temperature range. Holmes [27] attributed this to the dislocation climb process. Pahutova et al. [26] interpreted their data on creep of Zr in the temperature range 673–1223 K and suggested that dislocation glide and climb–glide is the rate controlling mechanism. The activation energy for creep for Zr–2.5Nb in the temperature region 573–673 K has been reported to be in the range of 209–261 kJ/mol [32].

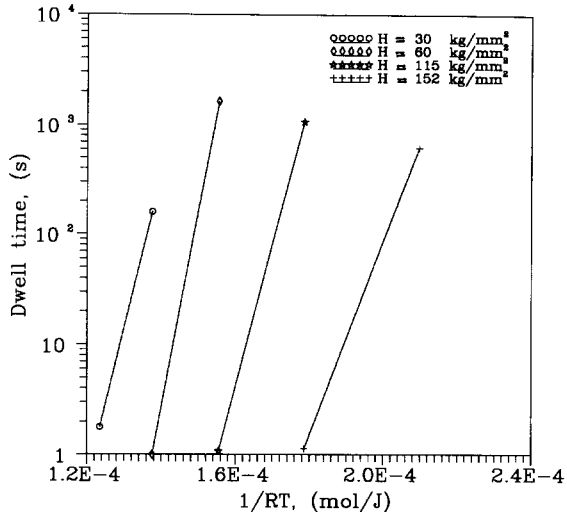


Fig. 6. ln(dwell time) versus $1/RT$ plot for the determination of activation energy for creep. The slope of these lines will be the activation energy.

The alloy content has a pronounced effect on the creep properties of zirconium alloys. Creep strength increases with alloying additions that interact and decrease the mobility of dislocations. In Zr alloys, the most effective strengthening mechanism is precipitation strengthening followed by substitutional strengthening [4]. The creep strength of Zr alloys was found to increase with increasing amount of Sn, Nb and Mo [33]. The atoms of these elements are smaller than the atom of Zr when present in solid solution and will interact with dislocations. Tin has the most beneficial effect on the creep strength because of its high solubility and effect in reducing the stacking fault energy in α-Zr [34]. Cr, Ni and Fe have a minor effect on creep strength because of their low solubility and lower atomic radius. Interstitials play a minor role in increasing the creep strength.

It is possible to examine the results obtained in this study from the above sighted observations. The creep parameters at different temperature regimes of the Zr–

Table 4
Creep parameters and mechanisms for Zr [22]

| Domain | Temperature (K) | Stress exponent | Activation energy (kJ/mol) | Probable mechanisms |
|---|---|---|---|---|
| 1 | 323–573 | 20–33 | 125–314 | dislocation intersection or interaction with $O_2$ atoms |
| 2 | 573–673 | 7.4 | 293 | non-conservative motion of jogs |
| 3 | 673–773 | 12 | 293–440 | dislocation interaction with impurities/precipitates |
| 4 | 773–973 | 6.3 | 276 | dislocation glide/diffusion controlled process |
| 5 | 973–1073 | 5.2 | 419 | formation and motion of divacancies/formation of thermal jogs |

1Nb–1Sn–0.1Fe alloy has been analyzed and the probable mechanism for each regime has been suggested as follows.

*4.3.1. 573–673 K*

The activation energy and stress exponent obtained in the temperature region 573–673 K for the Zr–1Nb–1Sn–0.1Fe alloy are 205 kJ/mol and ~42, respectively. Ramaswami and Craig [31] suggested that the plastic flow for pure Zr over this temperature range is not thermally activated. On the other hand, Gilbert et al. [22] suggested that the mechanism at this regime is thermally activated. To verify this, the hardness temperature data of the Zr–1Nb–1Sn–0.1Fe alloy has been replotted as the ratio of modulus corrected hardness, $(H/G)_T$, to that at room temperature, $(H/G)_{293}$. The shear modulus values of Zircaloy were taken from the literature [35] and used in this study. The $(H/G)_T/(H/G)_{293}$ versus temperature plot is shown in Fig. 3. It is seen from this plot, that the modulus corrected hardness ratio is independent of temperature in the temperature region 573–673 K. A similar athermal region has been reported for Zircaloy-2 in the temperature range 600–800 K when yield stress was plotted against temperature [36,37]. Hence creep deformation in this region is an athermal process as suggested for Zr by Ramaswami and Craig [31]. The mechanism suggested for this region is dislocation–interstitial interaction.

*4.3.2. 673–773 K*

Fig. 3 indicates that the corrected hardness ratio versus temperature plot in the temperature range 673–773 K is temperature dependant, contrary to the observation of Ramaswami and Craig [31] on Zr. Gilbert et al. [22] suggested that the deformation in this region is thermally activated, in agreement with our results. The activation energy obtained in this region is 297 kJ/mol and was found to be lower than the value for pure Zr in the same temperature range. The activation energy is very close to the activation energy for the diffusion of Sn in Zr matrix [38]. Li et al. [19] conducted indentation creep studies at a low temperature ($\sim 0.3T_m$) on a number of materials and suggested that the principal mechanism causing indentation creep is dislocation glide. Hence the mechanism suggested for this regime is dislocation glide.

*4.3.3. 773–873 K*

In the temperature range 773–873 K, a very high activation energy (418 kJ/mol) is obtained in this study. The stress exponent is in the range of 7–12. Warda et al. [30] had reported that α-Zr exhibits anomalous creep behaviour in the temperature range 723–823 K. The anomalies consist of abnormal responses to stress increment, spontaneous change in the creep rate and activation energy maxima. This behaviour has been consistent with the dynamic strain aging model. Since stress during the indentation process is very high ($> E/1000$, where $E$ is Young's modulus), the peak in the activation energy should shift to a lower temperature [28], as mentioned earlier. Hence the high activation energy obtained in this study can not be attributed to dynamic strain aging. Gilbert et al. [22] have obtained almost similar values of stress exponent and activation energy for Zr in the temperature range 673–773 K to that obtained in this study. They suggested that the mechanism for creep in this region is dislocation interaction with strong obstacles such as impurity clusters or precipitates, which is the most probable mechanism for the alloy investigated in this study.

*4.3.4. 873–973 K*

The temperature range 873–973 K, is characterized by a stress exponent of ~5 and an activation energy of 303 kJ/mol. The activation energy for Zr and Zircaloy-2 in the same temperature range is 276 and 272 kJ/mol, respectively [22,27]. Ardell and Sherby [25] reported a stress dependant activation energy for Zr in the above temperature range which increased from 214 to 327 kJ/mol with decreasing stress. Rosinger et al. [39], who conducted creep tests on Zircaloy-4 in the temperature range 940–1073 K, reported the value of $n$ and $Q$ as 5.3 and 285 kJ/mol, respectively. The value obtained in this study is very close to the values reported for Zr and Zircaloy and hence an identical mechanism is expected in this alloy. The probable mechanism in this temperature regime is the dislocation climb process.

To summarize, it has been noted from this experiment that creep parameters of the Zr–1Nb–1Sn–0.1Fe alloy are similar to that of other Zr alloys except in the temperature range 573–673 K where a higher value for the stress exponent is obtained for this alloy.

## 5. Conclusions

The hot hardness and indentation creep behaviour of the Zr–1Nb–1Sn–0.1Fe alloy have been evaluated in this study. The temperature dependence of experimentally observed hardness has been discussed in detail. The hardness versus temperature data for this alloy can be represented by the relationship $H = \kappa \exp(-BT)$. Hardness of the above alloy falls gradually up to the transition temperature (713 K) and on further heating decreases rapidly.

The stress exponent obtained from the hardness–time plot was found to decrease from ~42 at 573 K to ~5 at 973 K. The activation energy was also found to be temperature dependant.

At least four different domains of creep were observed for this alloy in the temperature range 573–973 K. The mechanism in the temperature range 573–673 K was found to be athermal. In the remaining domains the mechanism was found to be thermally activated.

The mechanism at different domains is explained with the help of activation parameters of pure zirconium and zirconium alloys.

## Acknowledgements

The authors wish to acknowledge Mr D.S.C. Purushotham, Head, Radiometallurgy Division, for permitting to publish this work and for his keen interest in this research programme. We also wish to record our sincere thanks to Mr E. Ramadasan and Dr J.K. Chakravarthy for enlightening discussion.

## References

[1] G.P. Sabol, G.R. Kilp, M.G. Balfour, E. Roberts, in: ASTM-STP-1023 (American Society for Testing Materials, Philadelphia, PA, 1989) p. 227.
[2] S.L. Wadekar, S. Ganguly, G.K. Dey, J.K. Chakravarthy, V. Chopra, P. Pandey, in: Proc. Int. Conf. on Physical Metallurgy (ICPM 94), eds. S. Banerjee and R. Ramanujam (Gordon Breach, Amsterdam, 1996) p. 443.
[3] K. Balaramamurthy, in: Proc. on Zirconium Alloys for Reactor Components (ZARC-91), Department of Atomic Energy, Bombay, 1991, p. K-1.
[4] D.G. Franklin, G.E. Lucas, A.L. Bement, in: ASTM-STP-815 (American Society for Testing Materials, Philadelphia, PA) p. 16.
[5] P. Rodriguez, in: Proc. on Zirconium Alloys for Reactor Components (ZARC-91), Department of Atomic Energy, Bombay, 1991, p. 46.
[6] E.R. Petty, H. O'neill, Metallurgia 63 (1961) 25.
[7] A.G. Atkins, D. Tabor, Proc. R. Soc. London Ser. A292 (1966) 441.
[8] D. Tabor, Rev. Phys. Technol. 1 (1970) 145.
[9] K. Ito, Sci. Rep. Tohoku Imp. Univ. 112 (1923) 137.
[10] V.P. Shishokin, Z. Anorg. Chem. 189 (1930) 263.
[11] J.H. Westbrook, Trans. Am. Soc. Met. 45 (1953) 221.
[12] H.D. Merchant, G.S. Murthy, S.N. Bahadur, L.T. Dwivedi, Y. Mehrotra, J. Mater. Sci. 8 (1973) 437.
[13] S.G. Song, G.T. Gray III, Metall. Trans. 26A (1995) 2665.
[14] J.K. Charavarthy, in: PhD thesis, Indian Institute of Science, Bangalore (1992) p. 4.
[15] W.W. Walker, in: The Science of Hardness Testing and its Research Applications, eds. J.H. Westbrook and H. Conard (Ameican Society for Metals, Metals Park, OH, 1973) p. 258.
[16] A.G. Atkins, A. Silverio, D. Tabor, J. Inst. Met. 94 (1966) 369.
[17] T.O. Mulhearm, D. Tabor, J. Inst. Met. 89 (1960–1961) 7.
[18] J.R. Mathews, Acta Metall. 28 (1980) 311.
[19] W.B. Li, J.L. Henshall, R.M. Hooper, K.E. Easterling, Acta Metall. Mater. 39 (1991) 3099.
[20] O. Prakash, D.R.H. Jones, Acta Mater. 44 (1996) 891.
[21] P.M. Sargent, M.F. Ashby, Mater. Sci. Technol 8 (1992) 594.
[22] E.R. Gilbert, S.A. Duran, A.L. Bement, in: ASTM-STP-458 (American Society for Testing Materials, Philadelphia, PA, 1969) p. 210.
[23] F.R. Shober, J.A. Van Echo, L.L. Marsh, J.R. Keeler, Battelle Memorial Institute Report No. BMI-1168, 1957.
[24] I.M. Bernstein, Trans. AIME 239 (1967) 1518.
[25] A.J. Ardell, O.D. Sherby, Trans. AIME 239 (1967) 1547.
[26] M. Pahutova, J. Cadek, V. Cerny, J. Nucl. Mater. 68 (1977) 111.
[27] J.J. Holmes, J. Nucl. Mater. 13 (1964) 137.
[28] D.G. Franklin, G.E. Lucas, A.L. Bement, in: ASTM-STP-815 (American Society for Testing Materials, Philadelphia, PA, 1983) p. 16.
[29] V. Fidleris, in: ASTM-STP-458 (American Society for Testing Materials, Philadelphia, PA, 1969) p. 1.
[30] R.D. Warda, V. Fidleris, E. Teghtsoonian, Metall. Trans. 4 (1973) 1201.
[31] B. Ramaswami, G.B. Craig, Trans. AIME 239 (1967) 1226.
[32] E.R. Gilbert, J. Nucl. Mater. 26 (1968) 105.
[33] W.A. McInteer, D.L. Baty, K.O. Stein, in: ASTM-STP-1023 (American Society for Testing Materials, Philadelphia, 1989) p. 621.
[34] G.M. Hood, T. Laursen, J.A. Jackman, R. Blec, R.J. Schultz, J.L. Whitton, Philos. Mag. 63A (1991) 937.
[35] D.O. Northwood, I.M. London, L.E. Bahen, J. Nucl. Mater. 55 (1975) 299.
[36] W. Tyson, J. Nucl. Mater. 24 (1967) 101.
[37] L.S. Rubenstein, J.G. Godwin, F.L. Shubert, Trans. Am. Soc. Met. 54 (1961) 20.
[38] M.C. Naik, R.P. Agarwala, Acta Metall. 15 (1967) 1521.
[39] H.C. Rosinger, P.C. Bera, W.R. Clendening, J. Nucl. Mater. 82 (1979) 286.